0022-3565/10/3323-710–719$20.00
THE JOURNAL OF PHARMACOLOGY AND EXPERIMENTAL THERAPEUTICS
JPET 332:710–719, 2010

Vol. 332, No. 3
162701/3563778
Printed in U.S.A.

Ligand-Induced Regulation and Localization of Cannabinoid CB_1 and Dopamine D_{2L} Receptor Heterodimers[S]

Julie A. Przybyla and Val J. Watts

Department of Medicinal Chemistry and Molecular Pharmacology, Purdue University, West Lafayette, Indiana

Received November 2, 2009; accepted December 15, 2009

ABSTRACT

The cannabinoid CB_1 (CB_1) and dopamine D_2 (D_2) receptors are coexpressed in the basal ganglia, an area of the brain involved in such processes as cognition, motor function, and emotional control. Several lines of evidence suggest that CB_1 and D_2 receptors may oligomerize, providing a unique pharmacology in vitro and in vivo. However, limited information exists on the regulation of CB_1 and D_2 receptor dimers. We used a novel technique, multicolor bimolecular fluorescence complementation (MBiFC) to examine the subcellular localization of CB_1-D_{2L} heterodimers as well as D_{2L}-D_{2L} homodimers in a neuronal cell model, Cath. a differentiated cells. MBiFC was then used to explore the effects of persistent ligand treatment on receptor dimerization at the plasma membrane and intracellularly. Persistent (20-h) agonist treatment resulted in increased formation of CB_1-D_{2L} heterodimers relative to the D_{2L}-D_{2L} homodimers. The effects of the D_2 agonist quinpirole were restricted to the intracellular compartment and may reflect increased D_{2L} receptor expression. In contrast, treatment with the CB_1 receptor agonist (2)-*cis*-3-[2-hydroxy-4-(1,1-dimethylheptyl)phenyl]-*trans*-4-(3-hydroxypropyl) cyclohexanol (CP55, 940) produced increases in both membrane and intracellular CB_1-D_{2L} heterodimers independently of alterations in CB_1 receptor expression. The effects of CB_1 receptor activation were attenuated by the CB_1 antagonist 1-(2,4-dichlorophenyl)-5-(4-iodophenyl)-4-methyl-*N*-4-morpholinyl-1*H*-pyrazole-3-carboxamide (AM281) and were both time- and dose-dependent. The effects of CB_1 activation were examined further by combining MBiFC with a constitutively active CB_1 receptor mutant, CB_1T210I. These studies demonstrated that the expression of CB_1T210I increased intracellular CB_1-D_{2L} heterodimer formation. In summary, agonist-induced modulation of CB_1-D_{2L} oligomerization may have physiological implications in diseases such as Parkinson's disease and drug abuse.

Increasing evidence suggests that G protein-coupled receptors (GPCRs) may function in receptor dimeric or higher order oligomeric complexes (for review, see Milligan, 2008). One set of receptors that has received significant attention relevant to oligomerization is the CB_1 cannabinoid (CB_1) receptor and dopamine D_2 (D_2) receptor (for review, see Fuxe et al., 2008). It is thought that the cannabinoid system negatively modulates dopamine circuits as activation of the CB_1 receptor leads to an attenuation of dopamine signaling (Laviolette and Grace, 2006). The CB_1 receptor is widely expressed in the central nervous system, with great abundance in the basal ganglia (Herkenham et al., 1991). CB_1 receptors are located on striatal GABAergic neurons (Herkenham et al., 1991), and they are also found on dendrites in both the dorsal striatum and the nucleus accumbens (Pickel et al., 2006). The D_2 receptor exists as two splice variants, D_{2S} (short) and D_{2L} (long). The D_{2S} variant is highly expressed on presynaptic dopaminergic neurons, whereas the D_{2L} variant is found postsynaptically on dopaminergic neurons throughout the striatum

This work was supported by the National Institutes of Health National Institute of Mental Health [Grant MH060397]; and the Purdue Research Foundation and the Department of Medicinal Chemistry and Molecular Pharmacology, Purdue University.

Article, publication date, and citation information can be found at http://jpet.aspetjournals.org.

doi:10.1124/jpet.109.162701.

[S] The online version of this article (available at http://jpet.aspetjournals.org) contains supplemental material.

ABBREVIATIONS: GPCR, G protein-coupled receptor; CB_1, cannabinoid 1 receptor; CC, Cerulean C-terminal fragment; D_2, dopamine D_2 receptor; D_{2S}, short form of D_2 receptor; D_{2L}, long form of D_2 receptor; FRET, fluorescence resonance energy transfer; BRET, bioluminescence resonance energy transfer; BiFC, bimolecular fluorescence complementation; BRET, bioluminescence resonance energy transfer; MBiFC, multicolor bimolecular fluorescence complementation; CAD, Cath. a differentiated; CP55,940, (2)-*cis*-3-[2-hydroxy-4-(1,1-dimethylheptyl)phenyl]-*trans*-4-(3-hydroxypropyl) cyclohexanol; SR141716A, *N*-(piperidin-1-yl)-5-(4-chlorophenyl)-1-(2,4-dichlorophenyl)-4-methyl-1*H*-pyrazole-3-carboximide hydrochloride; YFP, yellow fluorescent protein; PCR, polymerase chain reaction; PBS, phosphate-buffered saline; CFP, cyan fluorescent protein; VN, Venus N-terminal fragment; CN, Cerulean N-terminal fragment; CC, C-terminal fragment of Cerulean; cFRET, corrected fluorescence resonance energy transfer; M, muscarinic receptor; A_{2A} adenosine$_{2A}$ receptor; AM281, 1-(2,4-dichlorophenyl)-5-(4-iodophenyl)-4-methyl-*N*-4-morpholinyl-1*H*-pyrazole-3-carboxamide; ER, endoplasmic reticulum; wt, wild type.

(Khan et al., 1998; Usiello et al., 2000).[1] These observations reveal that CB_1 and D_{2L} receptors have overlapping expression patterns in the striatum and also suggest that they are colocalized in neurons in the nucleus accumbens (see references within Kearn et al., 2005; Pickel et al., 2006).

It has been reported that CB_1 and D_2 receptors oligomerize, providing unique pharmacology in vitro and in vivo (Glass and Felder, 1997; Jarrahian et al., 2004; Kearn et al., 2005; Marcellino et al., 2008). For example, it was demonstrated in primary rat striatal neurons that concurrent activation of $G\alpha_{i/o}$-coupled CB_1 and D_2 receptors resulted in stimulation of cAMP accumulation (Glass and Felder, 1997). Subsequent experiments using recombinant CB_1 and D_{2L} receptors suggested that D_{2L} receptor activation promoted a switch in CB_1 receptor coupling from $G\alpha_{i/o}$ to $G\alpha_s$ (Glass and Felder, 1997). One proposed mechanism for D_2 receptor modulation of CB_1-G protein coupling may involve receptor oligomerization. This hypothesis was examined by demonstrating a physical interaction between CB_1 and D_{2L} receptors using coimmunoprecipitation (Kearn et al., 2005). The same investigators also revealed that the CB_1-D_{2L} receptor complex can be dynamically modulated by receptor agonists. More recent studies have examined CB_1-D_{2L} heteromers using FRET techniques (Marcellino et al., 2008). Using human embryonic kidney cells transiently transfected with fluorescently tagged CB_1 and D_{2L} receptors, a FRET interaction was detected. However, no significant changes in the FRET signal were detected after short-term exposure to CB_1 or D_{2L} receptor agonists (Marcellino et al., 2008). The ability of CB_1 and D_{2L} receptors to interact is consistent with suggestion of a CB_1-D_{2L} heterodimer. Additional behavior and biochemical data support further the physiological relevance of CB_1 and D_2 receptors heterodimers (Fuxe et al., 2008). However, limited information exists on the cellular localization and regulation of CB_1-D_{2L} receptor heterodimers. Despite the therapeutic potential of drugs targeting these receptors, the effect of persistent receptor activation on the dynamics of receptor oligomerization has not been explored.

The most common techniques currently being used to study the physical association of GPCRs include coimmunoprecipitation and traditional resonance energy transfer (FRET and BRET) techniques (Vidi and Watts, 2009). These techniques are typically limited to the study of a single protein-protein complex. In addition, coimmunoprecipitation does not allow for detection of an interacting protein complex within a living cell. To gain further insight into GPCR dimerization in live cells, we recently established the use of multicolor bimolecular fluorescence complementation (MBiFC) (Hu et al., 2002; Shyu et al., 2006) as a tool to investigate GPCR homo- and heteromer oligomerization (Vidi et al., 2008a,b). MBiFC allows for the detection of two separate protein-protein complexes in living cells by visualizing the fluorescence complementation of two distinct spectral variants of green fluorescent protein (Hu and Kerppola, 2003). Moreover, this technique can be used to measure the relative amounts of homodimer versus heterodimer formation in a cell region-specific manner (Vidi et al., 2008b).

The present study uses MBiFC to examine CB_1-D_{2L} heterodimers and D_{2L}-D_{2L} homodimers in Cath. a differentiated (CAD) cells. CAD cells are a neuronal cell model that express GAP-43, synaptotagmin, and synaptosome-associated protein of 25 kDa and upon differentiation, form neurite-like processes (Qi et al., 1997). The present results provide additional evidence for the existence of CB_1 and D_{2L} receptor oligomers. We also revealed that persistent agonist (i.e., dopaminergic or cannabinergic) treatment favors the formation of the CB_1-D_{2L} heterodimer relative to the formation of the D_{2L}-D_{2L} homodimer. The D_2 agonist-mediated effects were accompanied by an increase in D_{2L} receptor expression, whereas the CB_1 agonist-mediated changes in heterodimer formation appeared to involve primarily CB_1 receptor activation. These results provide further insight into the dynamic nature of CB_1-D_{2L} oligomerization.

Materials and Methods

Materials. Human CB_1 and D_{2L} cDNAs were obtained from the Missouri S&T cDNA Resource Center (Rolla, MO). Growth media (Dulbecco's modified Eagle's medium), quinpirole, and sulpiride were obtained from Sigma-Aldrich (St. Louis, MO). Fetal bovine serum and bovine calf serum were purchased from Thermo Fisher Scientific (Waltham, MA). Penicillin/streptomycin/amphotericin B antibiotic/antimycotic was purchased from Invitrogen (Carlsbad, CA). Forskolin was purchased from Tocris Bioscience (Ellisville, MO). CP55,940 was a generous gift from Pfizer Pharmaceuticals (New York, NY). [^{3}H]cAMP (25 Ci/mmol) was purchased from PerkinElmer Life and Analytical Sciences (Boston, MA). [^{3}H]Spiperone (91 Ci/mmol) and [^{3}H]SR141716A (42 Ci/mmol) were obtained from GE Healthcare (Chalfont St. Giles, Buckinghamshire, UK). Specific cellular compartment markers (mCherry-mem, YFP-ER, YFP-Endo, and YFP-Golgi) were gifts from Dr. Catherine Berlot (Weis Center for Research, Danville, PA).

Expression Vectors. Full-length human CB_1 and D_{2L} cDNAs were amplified by polymerase chain reaction (PCR) using oligonucleotides with EcoRI, XbaI, or XhoI restriction sites and omitting the stop codons. The PCR products were digested with either EcoRI/XbaI or EcoRI/XhoI and ligated into the corresponding pBiFC vectors. These expression vectors contain nonfluorescent fragments of the N and C termini of the enhanced yellow fluorescent protein (Venus) and the enhanced cyan fluorescent protein (Cerulean). The N-terminal fragments (VN or CN) include residues 1 to 172, whereas the C-terminal fragment of Cerulean (CC) includes residues 155 to 238. This cloning strategy places the fragment on the C terminus of the receptors. In addition, the CB_1 and D_{2L} receptor PCR products were digested with either EcoRI/XbaI or EcoRI/XhoI and ligated into expression vectors containing the full-length Venus or Cerulean proteins resulting in the CB_1 and D_{2L} receptors tagged at the C terminus with either Venus or Cerulean. The CB_1 receptor mutant (CB_1T210I) was generated using the QuikChange kit according to the supplier's protocol (Stratagene, La Jolla, CA) in pcDNA3-CB_1 and then subcloned into the pBiFC vectors using EcoRI and XbaI restriction enzyme sites. All constructs were verified by DNA sequencing.

Cell Culture and Transient Transfections. CAD cells were maintained as described previously (Vortherms and Watts, 2004). For microscopic evaluation of BiFC, CAD cells were grown to approximately 70% confluence in four-well LabTek chambered coverslips (Nalge Nunc International, Rochester, NY). Cells were transfected with 1 μl of Lipofectamine 2000 (Invitrogen) according to the manufacturer's recommendations. In MBiFC experiments, CB_1-VN (500 ng), D_{2L}-CC (300 ng), and D_{2L}-CN (300 ng) were transiently cotrans-

[1] Personal communications confirmed that the D2L receptor was used in Glass and Felder (1997) (per Dr. David Sibley, who supplied the CHO-D2 cells) as well as in Marcellino et al. (2008) (per Dr. Kjell Fuxe).

fected with 20 ng of either mCherry-Mem, YFP-Endo, YFP-ER, or YFP-Golgi depending on the experiment. Twenty-four hours after transfection, the growth media and transfection reagent were replaced with 400 μl of warm phosphate-buffered saline (PBS), and images were taken using a charge-coupled device camera mounted on a TE2000-U inverted fluorescence microscope (Nikon, Melville, NY) equipped with a 100-W mercury lamp and band-pass filters (Chroma Technology Corp., Rockingham, VT) for Venus (excitation at 500/20 nm; emission at 535/30 nm), Cerulean (excitation, 430/25 nm; emission, 470/30 nm), or mCherry (Texas Red, excitation, 572/23 nm; emission, 625/25 nm). Fluorescent images were acquired using MetaMorph software (Molecular Devices, Sunnyvale, CA). For MBiFC experiments investigating the effects of receptor ligands on receptor dimer population, the cells were transfected as described above and 4 h after transfection, the appropriate drug treatment was added to the growth medium for an additional 20 h before image acquisition.

Quantitative Image Analysis. Quantification of fluorescent signals was performed as described previously using ImageJ software (http://rsb.info.nih.gov/ij/; Hu et al., 2002; Supplemental Fig. 1). In each experiment, approximately 40 to 50 individual cells were quantified. Ten microscopic fields at 60× magnification were acquired as stacks of images from the YFP, CFP, and Texas Red channels corresponding to the fluorescent signals from Venus, Cerulean, and mCherry proteins, respectively. Background fluorescence intensity was measured in each channel in an area devoid of cells and subtracted from the fluorescent signals. The signals corrected for background fluorescence were then scaled to a factor equal to that of the inverse of the exposure time for each pixel intensity measurement. The images of the mCherry-Mem membrane marker signal were used to select cells for image analysis and to normalize BiFC signals (Supplemental Fig. 1). Cellular analysis of BiFC signals was performed in two parts. First, the fluorescent signal intensity maximum at the membrane was determined by drawing a perpendicular line through the membrane using the mCherry-Mem image. The maximum signal intensity was determined in all three channels, YFP, CFP, and Texas Red to estimate the BiFC signals at the membrane. The BiFC signal intensity in the intracellular space was determined by outlining the intracellular compartment (excluding the plasma membrane) and determining the average pixel intensity in all three channels, YFP, CFP, and Texas Red, to estimate the intracellular BiFC signals. Cells with saturated signals as well as cells with signals that were 1.2 times lower than background were not used for quantification. BiFC experiments assessing bleed-through/overflow of Cerulean or Venus in the opposite channels (i.e., YFP or CFP) revealed minimal cross-talk. Specifically, complemented Cerulean contributed less than 2% of the YFP signal and complemented Venus contributed less than 3% of the CFP signal (data not shown). Venus/Cerulean fluorescence ratios exhibit a non-Gaussian distribution; therefore, median values were calculated and averaged between experiments.

Cyclic AMP Accumulation Assays. CAD cells were grown to 70% confluence in 24-well plates and were transiently transfected as described previously (Vidi et al., 2008a). CAD cells were either transfected with 300 ng/well D_{2L} constructs or 500 ng/well CB_1 constructs. All drugs were diluted in Earle's balanced salt solution assay buffer (Earle's balanced salt solution containing 2% bovine calf serum, 0.025% ascorbic acid, and 15 mM HEPES, pH 7.4) and added to the cells on ice. Determination of cAMP accumulation was performed by incubating the transfected CAD cells with forskolin (10 μM) in the absence and presence of either CP55,940 (10 μM) or quinpirole (10 μM) for 15 min at 37°C. All assays were performed in the presence of the phosphodiesterase inhibitor 3-isobutyl-1-methylxanthine (500 μM) and terminated with ice-cold 3% trichloroacetic acid. Quantification of cAMP accumulation was determined using a competitive binding assay as described previously (Vortherms and Watts, 2004).

Radioligand Binding Assays. Single point radioligand binding assays were used to estimate CB_1 and D_{2L} receptor densities after drug treatments as described previously (Vidi et al., 2008a). CAD cells were plated in a 12-well plate and were grown to 70% confluence before being transiently transfected with CB_1-VN, D_{2L}-CN, and D_{2L}-CC using 2 μl/well of Lipofectamine 2000. Four hours after transfection, the appropriate drug treatment was added in triplicate to the growth medium and transfection reagent. The cells were incubated for an additional 20 h before single point radioligand binding assays. Cells were washed three times with 500 μl of receptor binding buffer (50 mM Tris and 4 mM $MgCl_2$, pH 7.4). The cells were lysed with 500 μl of ice-cold lysis buffer (1 mM HEPES and 2 mM EDTA, pH 7.4) for 10 min on ice. The cells were removed from each well by trituration, and crude cell membranes were collected by centrifugation (30,000*g* for 15 min at 4°C). Membrane pellets were resuspended by mechanical homogenization in 1 ml of receptor binding buffer. For CB_1 receptor binding, the addition of 0.5% bovine serum albumin to the receptor binding buffer was used to decrease nonspecific binding. Crude cell membranes (approximately 30 μg in 150 μl) were added in duplicate to the assay tubes to determine both nonspecific and total binding. For CB_1 binding, nonspecific binding was defined by 10 μM nonradioactive SR141716A (essentially identical levels of nonspecific binding were obtained using 10 μM AM281; data not shown). All tubes contained a near-saturating amount of [^{3}H]SR141716A (50 μl; final concentration, ~5.0 nM) in a total volume of 500 μl. Likewise, for D_2 binding, nonspecific binding was defined with 5 μM (+)-butaclamol, with all reaction conditions containing a near-saturating amount of [^{3}H]spiperone (50 μl; final concentration, ~1.5 nM) in a total volume of 500 μl. The reaction was terminated by filtration onto FB glass fiber plates with ice-cold wash buffer (10 mM Tris and 0.9% NaCl) using a cell harvester (FilterMate; PerkinElmer Life and Analytical Sciences). Radioactivity was determined a TopCount scintillation counter (PerkinElmer Life and Analytical Sciences). Specific binding was determined as the difference between the average of the nonspecific and total binding conditions. The specific binding amount was normalized to the amount of protein using the bicinchoninic acid protein assay (Pierce Chemical, Rockford, IL) following the supplier's protocol. Under the transfection conditions used to explore the effects of drug treatments on BiFC, the following estimated K_d and B_{max} values were obtained via radioligand saturation binding experiments: [^{3}H]SR141716A, K_d = 0.74 ± 0.18 nM and B_{max} = 204 ± 28 fmol/mg; and [^{3}H]spiperone, K_d = 0.051 ± 0.02 nM and B_{max} = 3550 ± 200 fmol/mg.

Fluorescence Energy Transfer. CAD cells were grown to 70% confluence in 12-well plates before transfection. Cells were transiently transfected with three general conditions depending on the receptor dimer species to be studied including: cells only expressing the FRET donor (Cerulean), cells only expressing the FRET acceptor (Venus), and cells expressing both the donor and acceptor. To normalize for protein expression in cells only expressing either the donor or acceptor, the total amount of DNA transfected was normalized with the untagged receptor. In each FRET assay, 750 ng/well of the donor (CB_1-Cerulean or D_{2L}-Cerulean) and 750 ng/well of the acceptor (CB_1-Venus or D_{2L}-Venus) were transiently transfected either alone or in combination 24 h before the experiment. Cells were washed with 500 μl of warm PBS and resuspended in 300 μl of warm PBS. Protein concentration was determined on the cell suspension using the bicinchoninic acid assay method (Pierce Chemical) and normalized to 200 ng/μl with PBS. CAD cells suspensions (40 μg) were transferred into a 96-well black plate (Nalge Nunc International), and fluorescence measurements were evaluated on the FUSION plate reader (PerkinElmer Life and Analytical Sciences). Determination of FRET signals was performed as described previously (Vidi et al., 2008b). In brief, FRET signals were measured using the sensitized acceptor method. Mock-transfected cells were used for background fluorescence. For each sample, Cerulean (C) and Venus (V) was measured using 430/25 nm and 500/20 nm excitation and 470/30 nm and 535/30 nm emission filters. FRET signals (F) were measured using excitation at 430/25 nm and emission at 535/30 nm. Bleed-through coefficients were calculated for the acceptor ($a = F/V$) and for the donor ($d = F/C$)

in cells only expressing either Cerulean (donor) or Venus (acceptor) fusion proteins. The FRET signals were corrected (cFRET) for acceptor and donor bleed-through using the equation $cFRET = F - aV - dC$. The signals were then normalized to donor (C) and acceptor (Y) intensities as follows: $nFRET = cFRET/\sqrt{C \times V}$.

Data and Statistical Analysis. Data and statistical analyses were performed using Prism (GraphPad Software Inc., San Diego, CA). A p value <0.05 was considered significant.

Results

Functional cAMP accumulation assays were performed to verify the signaling properties of the BiFC-tagged CB_1 and D_{2L} receptors (Fig. 1). Because CB_1 and D_{2L} receptors couple to inhibitory G proteins (i.e., $G\alpha_{i/o}$), agonist-induced inhibition of forskolin-stimulated cAMP accumulation was used to evaluate receptor function. The BiFC-tagged D_{2L} receptors D_{2L}-CN and D_{2L}-CC were functional after stimulation with the D_2 agonist quinpirole (10 μM), revealing approximately 60% inhibition of forskolin-stimulated cAMP accumulation (Fig. 1A). Additional experiments confirming the functionality of the BiFC-tagged CB_1 receptors, CB_1-VN and CB_1-CC, were performed. Both constructs were functional after stimulation with the CB_1 receptor agonist CP55,940 (10 μM), yielding more than 35% inhibition of forskolin-stimulated cAMP accumulation (Fig. 1B). A modest but insignificant degree (approximately 10%) of inhibition was also observed in vector-transfected CAD cells. Receptor signaling in cells coexpressing the wild-type or BiFC-tagged receptors was also examined (Fig. 1, A and B). The D_2 agonist quinpirole robustly inhibited forskolin-stimulated cAMP accumulation in cells coexpressing CB_1 and D_{2L} receptors (CB_1 + D_{2L} or CB_1-VN + D_{2L}-CC) as well as cells cotransfected with D_{2L}-CN and D_{2L}-CC. Similar experiments revealed that CP55,940, inhibited forskolin-stimulated cAMP accumulation in cells coexpressing CB_1 and D_{2L} receptors (CB_1 + D_{2L} and CB_1-VN + D_{2L}-CC). These data suggest that the addition of a C-terminal tag (-VN, -CN, or -CC) and fluorescence complementation (see below) do not adversely affect agonist-mediated inhibition of cAMP accumulation.

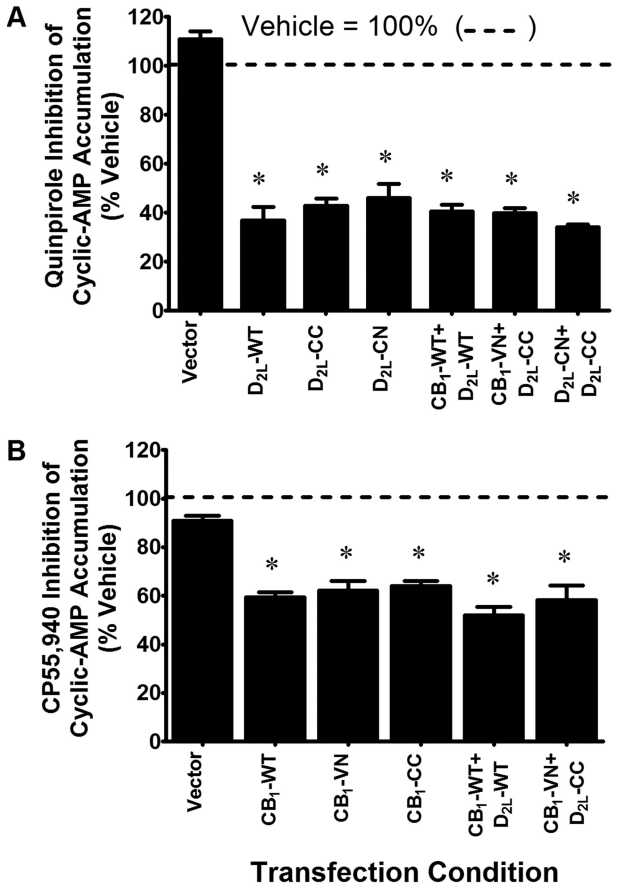

Fig. 1. Functional characterization of receptor-BiFC fragment fusion proteins by measurement of acute inhibition of forskolin-stimulated cAMP accumulation. CAD cells were transiently transfected as indicated. Cyclic AMP accumulation was measured after a 15-min incubation with forskolin (10 μM) in the presence of quinpirole (10 μM) (A) or CP55,940 (10 μM; B) as shown. All data are normalized to the percentage of forskolin-stimulated cAMP accumulation under matched transfection conditions. Each bar represents the mean ± S.E.M. of three to four independent experiments assayed in duplicate. *, $p < 0.05$ compared with forskolin-stimulated cAMP accumulation under vehicle conditions (one-sample t test).

MBiFC is novel technique that allows for the simultaneous study of two receptor dimer species within living cells (Fig. 2A; Vidi and Watts, 2009). Initial single color BiFC experiments used the fusion receptors to confirm interactions between CB_1 and D_{2L} receptors. Coexpression of either combination of BiFC constructs (CB_1-VN + D_{2L}-CC or D_{2L}-VN + CB_1-CC) in CAD cells produced a robust Venus signal (Supplemental Fig. 2A). Additional BiFC studies compared the CB_1-D_{2L} fluorescent signal with CB_1 or D_{2L} receptors in combination with the M_4 muscarinic receptor BiFC constructs (i.e., CB_1-VN + M_4-CC or D_{2L}-CC + M_4-VN). The CB_1-D_{2L} heterodimer displayed an enhanced fluorescent signal compared with the M_4-containing heterodimers (Supplemental Fig. 2B). The formation of CB_1-D_{2L} heterodimers supports previous studies demonstrating interactions between CB_1 and D_{2L} receptors (Kearn et al., 2005; Marcellino et al., 2008).

One goal of the present study was to assess the dynamic nature of the CB_1-D_{2L} heterodimer in response to persistent drug treatment. This required the establishment of MBiFC as described previously for A_{2A} adenosine and D_{2L} dopamine receptors (Vidi et al., 2008a). Using this approach, CAD cells were transiently transfected with CB_1-VN, D_{2L}-CC, and D_{2L}-CN to simultaneously visualize CB_1-D_{2L} and D_{2L}-D_{2L} receptor dimers using fluorescence microscopy (Fig. 2A). The presence of a Venus signal is indicative of the CB_1-D_{2L} heterodimer, whereas a Cerulean signal corresponds to the D_{2L}-D_{2L} homodimer (Fig. 2B). CAD cells transfected with CB_1-VN, D_{2L}-CC, and D_{2L}-CN expressed both Venus and Cerulean signals consistent with the coexistence of CB_1-D_{2L} heterodimers and D_{2L}-D_{2L} homodimers (Fig. 2B). Fluorescent signals corresponding to the receptor dimers showed a similar pattern of distribution and were found at the plasma membrane as well as intracellularly. For comparison with the BiFC signals, the localization patterns of CB_1-Venus and D_{2L}-Cerulean were evaluated after coexpression (Fig. 2C). The CB_1-Venus signal showed significant intracellular localization, whereas the D_{2L}-Cerulean displayed localization at both the plasma membrane and intracellular compartments. Moderate overlap between the CB_1 and D_{2L} signals was also observed. For additional comparison, the individual expression patterns of CB_1-Venus and D_{2L}-Venus were examined (Fig. 2D). When expressed alone, the CB_1-Venus signal was primarily localized intracellularly demonstrated by the lack of overlap with the membrane marker (merge panel). Conversely, the D_{2L}-Venus expression was found primarily at the

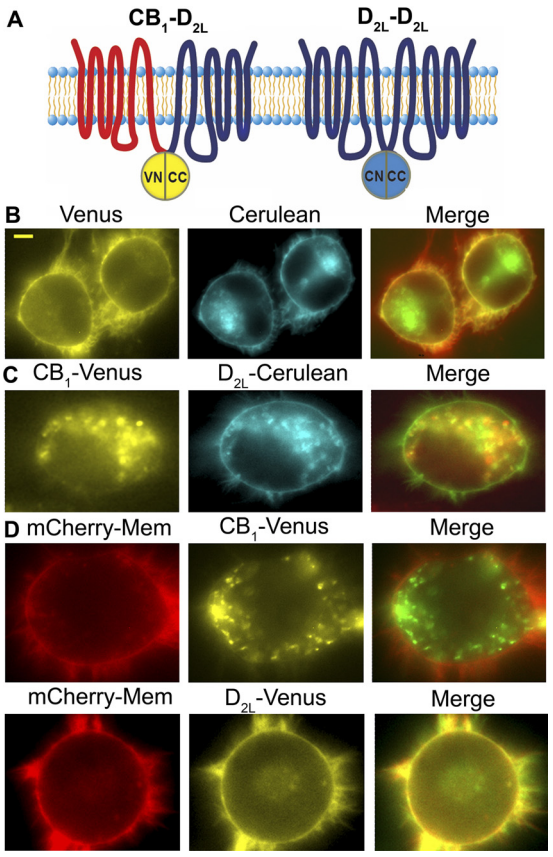

Fig. 2. CB_1-D_{2L} and D_{2L}-D_{2L} dimers detected by MBiFC. A, schematic representing the MBiFC approach used in these studies. CB_1-D_{2L} dimerization reconstitutes the Venus fluorescent protein (yellow) and D_{2L}-D_{2L} dimerization reconstitutes the Cerulean fluorescent protein (cyan). B, representative images of the fluorescent signals observed in an MBiFC study as described in the schematic in A. CAD cells were transiently transfected and imaged as described under *Materials and Methods*. The merged image (overlapping signal in yellow) represents an overlap of the Venus signal (depicted in red) and the Cerulean signal (depicted in green). Scale bar, 5 μm. C, representative images of the expression patterns of CB_1-Venus and D_{2L}-Cerulean receptors after cotransfection. The merged image (overlapping signal in yellow) represents an overlap of CB_1-Venus (depicted in red) and D_{2L}-Cerulean (depicted in green). D, representative images of the expression patterns of CB_1-Venus (top) and D_{2L}-Cerulean (bottom) after individual transfections in the presence of mCherry-mem. The merge image (overlapping signal in yellow) represents the overlap of either CB_1-Venus or D_{2L}-Venus (green signal) with mCherry-mem (red signal).

membrane and extensive overlap with the membrane marker was displayed (Fig. 2D).

We also attempted to perform MBiFC experiments to simultaneously examine D_{2L}-CB_1 and CB_1-CB_1 dimers. Unfortunately, the fluorescent signal of the CB_1-CB_1 dimer under MBiFC conditions was too low to reliably measure, restricting our MBiFC experiments to CB_1-D_{2L} and D_{2L}-D_{2L} receptor dimers. The lack of a CB_1-CB_1 dimer BiFC signal may reflect one of the disadvantages of BiFC. Specifically, the intensity of the fluorescence complementation signal is considerably weaker (2.5–5.5-fold) than the signal from the corresponding full-length fluorescent protein under similar transfection conditions (Vidi and Watts, 2009).

One advantage of BiFC is the ability to investigate the localization of the receptor dimers using epifluorescence. With the use of fluorescently tagged intracellular makers, the patterns of intracellular expression of the CB_1-D_{2L} and D_{2L}-D_{2L} receptor dimers were investigated using fluorescent microscopy (Fig. 3). CAD cells were transiently transfected with BiFC constructs that reconstitute Cerulean to either express the CB_1-D_{2L} heterodimer (CB_1-CN + D_{2L}-CC) or the D_{2L}-D_{2L} homodimer (D_{2L}-CN + D_{2L}-CC). In addition, these cells were transfected with the indicated YFP-tagged intracellular marker proteins (YFP-Endo, YFP-ER, or YFP-Golgi; Fig. 3). The endosome marker (YFP-Endo) is a fusion protein with RhoB, a known endosomal protein fused to YFP. The ER marker (YFP-ER) consists of YFP fused to the ER targeting sequence of calreticulin and the KEDL ER retrieval sequence. The Golgi marker (YFP-Golgi) is a YFP fusion protein with residues 1 to 81 of the β1,4-galactosyltransferase protein. Overall, both receptor dimers, D_{2L}-D_{2L} and CB_1-D_{2L} displayed moderate to extensive overlap with endosome and ER structures (Fig. 3, A and B). However, CB_1-D_{2L} and D_{2L}-D_{2L} receptor dimers demonstrated minimal to no overlap with the Golgi apparatus. These expression patterns are consistent with receptor dimer assembly at the ER (Herrick-Davis et al., 1997) and proper trafficking into endosomes (Leterrier et al., 2004). However, the additional possibility that receptors dimerize at the plasma membrane cannot be excluded in the absence of additional studies.

The results demonstrating MBiFC in neuronal cells were further validated by examining dimerization of these receptors

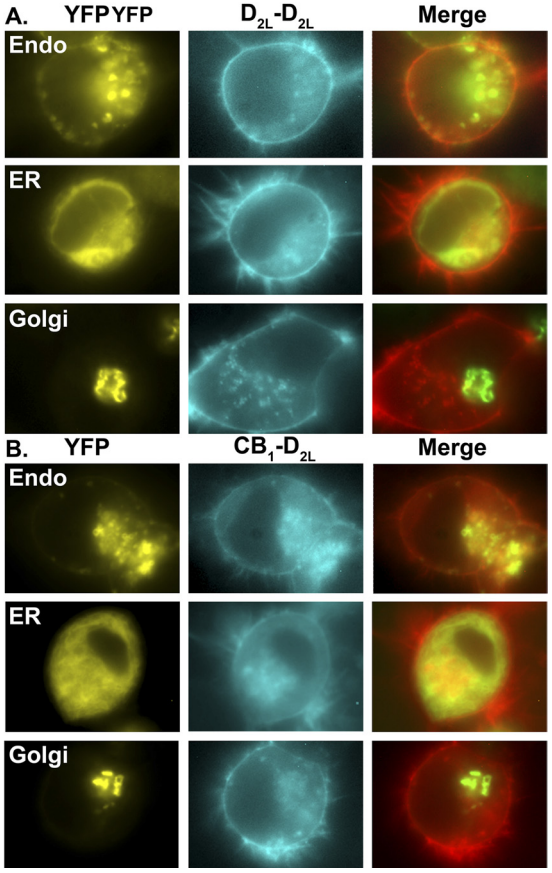

Fig. 3. Intracellular localization patterns of the D_{2L}-D_{2L} homomers and CB_1-D_{2L} heteromers. CAD cells were transiently transfected with both D_{2L}-CC and D_{2L}-CN (cyan signal in A) or CB_1-VN and D_{2L}-CC (cyan signal in B) along with the indicated YFP fluorescent marker proteins (yellow signal). The merged image (overlapping signal in yellow) represents an overlap of the BiFC signal (depicted in red) and the fluorescent marker signal (depicted in green). Images are representative of three independent transfections.

using FRET, which has been used previously to investigate interactions of CB_1 and D_{2L} receptors (Marcellino et al., 2008). CAD cells were transiently transfected with either CB_1-Venus + CB_1-Cerulean, CB_1-Venus + D_{2L}-Cerulean, or D_{2L}-Venus + D_{2L}-Cerulean (Fig. 4). A significant FRET signal was detected with all three receptor pairs compared with the mix control sample in which suspensions of cells only expressing the donor or acceptor was mixed in the FRET sample plate. These results provide further confirmation of our BiFC studies, supporting the hypothesis that CB_1 and D_2 form both homo- and heteromeric receptor oligomers in a neuronal-like cell model.

Using MBiFC and FRET techniques, we have provided evidence that CB_1 and D_2 receptors participate in receptor dimer complexes. We next sought to investigate the effects of persistent ligand treatment on the formation of CB_1 and D_{2L} heterodimer and D_{2L} homodimers using MBiFC as a tool to monitor changes in relative receptor dimer population. CAD cells were transiently transfected with CB_1-VN, D_{2L}-CC, and D_{2L}-CN, and the presence of the CB_1-D_{2L} heterodimer (Venus) and D_{2L}-D_{2L} homodimer (Cerulean) was simultaneously measured. The fluorescent intensity ratio of Venus to Cerulean in both the plasma membrane and intracellular compartments was determined after drug treatment. Under the conditions used, an increase in the Venus-to-Cerulean ratio would be indicative of an increase in the formation of the CB_1-D_{2L} receptor dimer relative to the D_{2L}-D_{2L} receptor dimer compared with vehicle-treated cells.

Our previous work with D_2 and A_{2A} receptor ligands suggested that a 20-h drug treatment provided a robust BiFC signal in which drug-induced changes in A_{2A}-D_{2L}, D_{2L}-D_{2L}, and A_{2A}-A_{2A} dimers could be observed (Vidi et al., 2008a). In the present study, we completed MBiFC time course experiments with the CB_1 receptor ligand CP55,940 to verify that a similar treatment duration produced robust responses in the absence of a ceiling effect. The results of the time course study revealed that CP55,940 treatments shorter than 10 h (i.e., 5 h) had very low fluorescent signals and did not allow us to quantify an adequate number of cells for analysis (data not shown). However, robust YFP and CFP signals were evident after 10 h and the drug effects were time-dependent showing the greatest response at 30 h (Fig. 5). The time course study also suggested

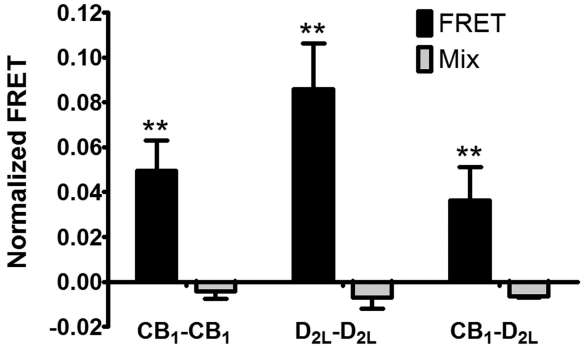

Fig. 4. CB_1 and D_{2L} receptor form homo- and heteromeric receptor oligomers as measured by FRET. CAD cells were transiently transfected with 750 ng/well of either CB_1-Venus and CB_1-Cerulean, D_{2L}-Venus and D_{2L}-Cerulean, or CB_1-Venus and D_{2L}-Cerulean. Mix samples represent a mixture of CAD cell suspensions individually expressing the respective fluorescently tagged receptors of interest. Data represent the mean ± S.E.M. of three independent experiments assayed in triplicate. **, $p < 0.01$ compared with mixed samples (one-way analysis of variance followed by Dunnett's post hoc test).

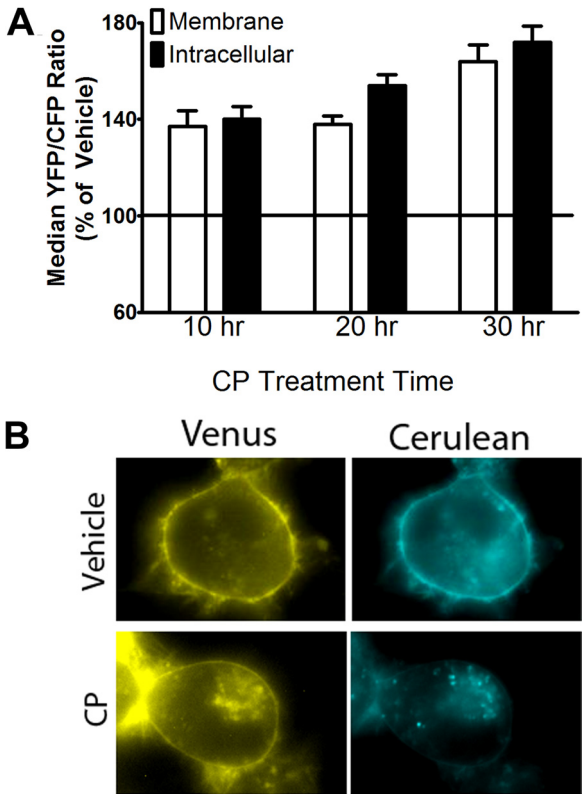

Fig. 5. Time course examining the effects of persistent CP55,940 treatment on heteromer (D_{2L}-CB_1-Venus) and homomer (D_{2L}-D_{2L}-Cerulean) formation. CAD cells were transiently transfected with CB_1-VN, D_{2L}-CC, and D_{2L}-CN followed by quantitative image analyses of the Venus/Cerulean ratios for the membrane and intracellular compartments. A, cells were incubated with 10 μM CP55,940 for 10, 20, or 30 h before image analysis. Data represents the average median Venus-to-Cerulean ratio values normalized to percentage of vehicle treatment (±S.E.M.) in four independent experiments. B, images from 20-h time point depicting the effects of CP55,940 on Venus and Cerulean signals.

that the 20-h time point is on the dynamic portion of the temporal scale potentially allowing us to observe ratiometric changes in both directions as shown previously (Vidi et al., 2008a). Examination of the overall YFP and CFP intensities at 20 h indicated that the CP55,940-induced increase in the YFP/CFP ratio reflected a combined increase in the YFP signal (CB_1-D_{2L}) and a decrease in the CFP signal (D_{2L}-D_{2L}) compared with vehicle-treated cells. Specifically, the membrane showed an 11% increase in YFP and a 27% decrease in CFP intensity. Intracellularly, there was 33% increase in the YFP signal and a 15% decrease in the CFP signal ($n = 4$).

Drug-induced changes in the relative receptor dimer population were measured after treatment (20 h) with either D_2 (Fig. 6A) or CB_1 (Fig. 6B) receptor ligands. Persistent activation of the D_{2L} receptor with quinpirole (10 μM) resulted in a significant increase in the Venus-to-Cerulean ratio consistent with an increase in CB_1-D_{2L} heterodimers relative to D_{2L}-D_{2L} homodimers. However, this effect was only significant in the intracellular compartment. The effect of quinpirole was prevented by coapplication of the selective D_2 receptor antagonist sulpiride (1 μM). Treatment with sulpiride alone or in combination with quinpirole resulted in a significant decrease in the Venus to Cerulean ratio in both the membrane and intracellular compartments. Because the observed alterations in receptor dimer population may involve changes in re-

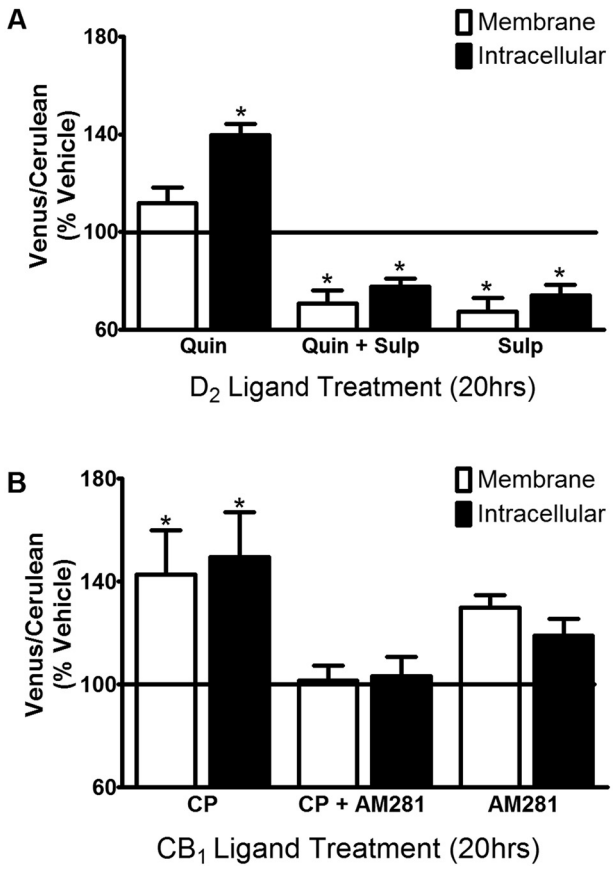

Fig. 6. Effects of persistent ligand treatment on heteromer (D_{2L}-CB_1-Venus) and homomer (D_{2L}-D_{2L}-Cerulean) formation. CAD cells were transiently transfected and imaged as described for Fig. 5. A, cells were incubated with 10 μM quinpirole (Quin), 1 μM sulpiride (Sulp), or quinpirole + sulpiride (Quin + Sulp) for 20 h. B, cells were incubated with 10 μM CP55,940 (CP), 10 μM AM281, or CP55,940 + AM281 (CP + AM281) for 20 h. Data represent the average median Venus-to-Cerulean ratio values normalized to percentage of vehicle treatment (± S.E.M.). *, $p < 0.05$ (compared with vehicle, one-sample t test, $n = 5–8$).

ceptor expression, single point radioligand binding experiments were used to estimate relative receptor densities after drug treatment. The results of these studies revealed that persistent treatment with quinpirole (10 μM), sulpiride (1 μM), or quinpirole + sulpiride significantly increased D_{2L} receptor density (118 ± 6, 149 ± 17, or 129 ± 9%; $n = 5$) compared with vehicle treatment (100%). These ligand-induced increases in D_{2L} receptor expression are consistent with our previous report (Vidi et al., 2008a) and work from others (Sibley and Neve, 1997). No significant changes in CB_1 receptor density were observed upon persistent treatment with either of the D_2 receptor ligands alone or the combination (data not shown).

MBiFC experiments were also performed using CB_1 ligands. Persistent treatment with the CB_1 receptor agonist CP55,940 (10 μM) led to a significant increase in the Venus-to-Cerulean ratio in both the plasma membrane and the intracellular regions compared with vehicle-treated cells (Fig. 6B). The addition of the CB_1 receptor antagonist AM281 (10 μM) attenuated the CP55,940-induced increase in the Venus-to-Cerulean ratio. Dose-response experiments revealed that the average EC_{50} values for CP55,940 increasing the YFP/CFP ratio were 320 and 210 nM for membrane and intracellular signals, respectively (Fig. 7). Subsequent single point radioligand binding experiments revealed that 20-h treatment with CP55,940 had no effect on CB_1 receptor density (106 ± 12%; $n = 5$); however, a modest decrease in D_{2L} receptor density (82 ± 3%; $n = 5$) was observed.

The observations described above suggest that persistent activation of the CB_1 receptor favors the formation of CB_1-D_{2L} heterodimers without alterations in CB_1 receptor expression. To investigate further the role of persistent activation on receptor dimerization, a constitutively active CB_1 receptor mutant was constructed for use in the MBiFC experiments. Threonine 210 of the CB_1 receptor was mutated to an isoleucine (CB_1T210I) to create a constitutively active receptor (D'Antona et al., 2006). The presence of an isoleucine at amino acid 210 disrupts the salt bridge in the DRY motif mimicking receptor activation, leading to enhanced agonist affinity and increased intracellular localization (D'Antona et al., 2006). We examined and compared the relative receptor heterodimer (CB_1-D_{2L}) and homodimer (D_{2L}-D_{2L}) populations in cells expressing either the wild-type (CB_1wt) or the constitutively active CB_1 receptor (CB_1T210I) using MBiFC (Fig. 8). The Venus- (CB_1-D_{2L}) to-Cerulean (D_{2L}-D_{2L}) ratios at the plasma membrane were similar in cells expressing the wild-type or constitutively active CB_1 (Fig. 8A). In contrast, expression of CB_1T210I resulted in a significant increase in the intracellular Venus-to-Cerulean ratio compared with the wild type CB_1 (Fig. 8A). The intracellular-to-membrane ratio of the Venus signal (i.e., CB_1wt-D_{2L} or T210I-D_{2L} dimer) in cells expressing the CB_1T210I mutant was also significantly increased (approximately 150%) compared with cells expressing CB_1wt (Fig. 8, A and B). The overlapping expression patterns of CB_1-D_{2L} and D_{2L}-D_{2L} dimers were markedly reduced in cells coexpressing CB_1T210I as indicated by a loss of white signal on the membrane in the merged images. Subsequent localization studies with the CB_1T210I-D_{2L} heterodimer revealed significant signal overlap with the endosomes and limited overlap in the ER consistent with enhanced endocytosis of the CB_1T210I mutant (D'Antona et al., 2006; Supplemental Fig. 3).

Discussion

Evidence for the existence and functional significance of CB_1 and D_{2L} heterodimers has continued to evolve over the

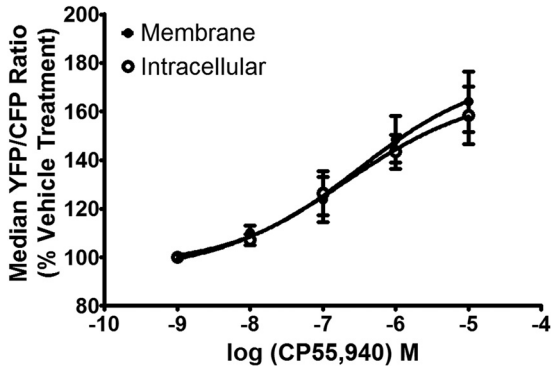

Fig. 7. Dose-response analysis for CP55,940 modulation of the Venus/Cerulean ratio. CAD cells were transiently transfected and imaged as described for Fig. 5. Cells were incubated with increasing concentrations of CP55,940 for 20 h. Data represent the average median Venus-to-Cerulean ratio values normalized to percentage of vehicle treatment (±S.E.M.) in three independent experiments.

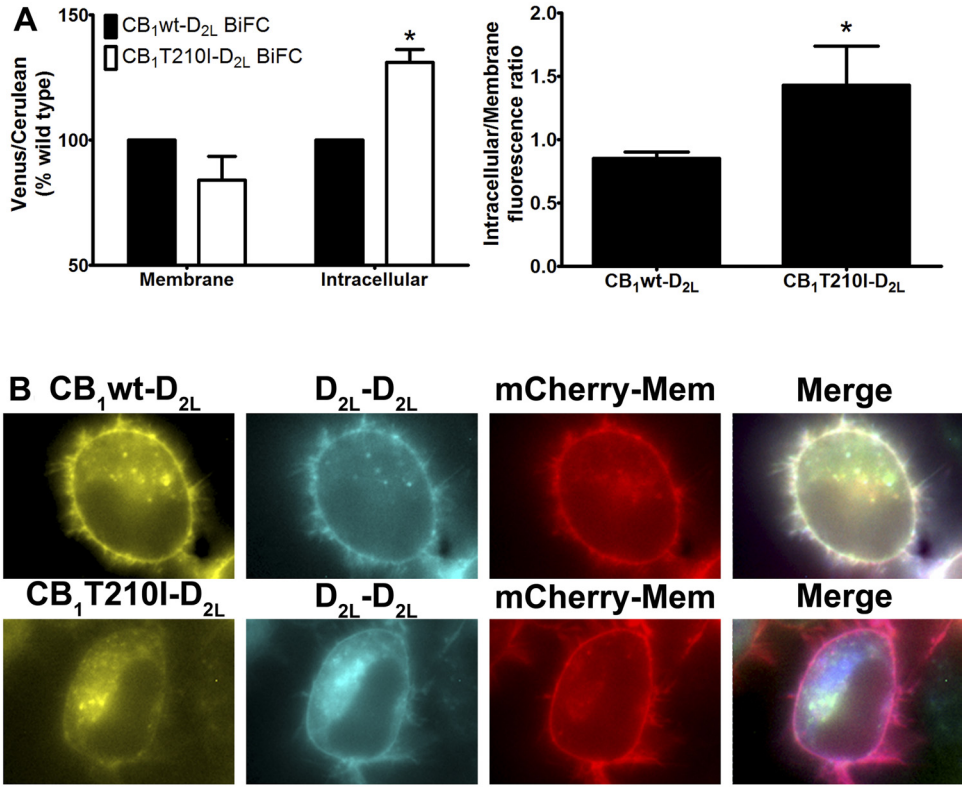

Fig. 8. Effect of constitutively active CB_1 receptor (T210I) on relative dimer population at the plasma membrane or intracellular compartment. CAD cells were transiently transfected with either CB_1wt-VN or CB_1T210I-VN with D_{2L}-CC and D_{2L}-CN. A, left, quantitative image analyses of the Venus/Cerulean ratios were determined for the membrane and intracellular compartments as described under *Materials and Methods*. The Venus-to-Cerulean ratio induced by CB_1T210I was normalized to the Venus-to-Cerulean ratio measured in cells expressing CB_1wt receptor; *, $p < 0.05$ (compared with wild type, one-sample t test). Right, quantitative image analyses of the intracellular/membrane ratios were determined for the CB_1-D_{2L}-Venus signal in cells either expressing CB_1wt or CB_1T210I. *, $p < 0.05$ (compared with wild type, t test). Data for both analyses were generated from the same experiments and represent the average median ± S.E.M. from three independent experiments. B, representative images of CAD cells expressing either CB_1wt (top) or CB_1T210I (bottom) to reconstitute the BiFC signals CB_1(wt or T210I)-D_{2L}-Venus and D_{2L}-D_{2L}-Cerulean and the membrane marker (mCherry-mem). The merge panel represents overlap of the three channels and overlapping pixel intensity is presented in white.

past 10 to 15 years. However, investigations examining the regulation of these heterodimers and their homodimer counterparts are just beginning as new technological advances for studying protein-protein interactions are developed (Vidi and Watts, 2009). In the present study, we have applied MBiFC as a novel technique to study the dimerization of CB_1 and D_{2L} receptors, and we reveal for the first time the localization patterns of these receptor heterodimers in a neuronal cell model.

Early studies of CB_1 and D_{2L} function were central to the development of the concept of CB_1-D_{2L} heterodimer (for review, see Glass et al., 1997). Several studies suggest that the CB_1-D_{2L} dimer possesses stimulatory properties toward adenylyl cyclase via the CB_1 receptor engaged in the heterodimer (Glass and Felder, 1997; Jarrahian et al., 2004; Kearn et al., 2005). However, conflicting conclusions from studies examining the regulation of CB_1 and D_{2L} receptor dimerization remain. One potential mechanism for regulating the CB_1-D_2 dimer is based on observations that the physical association of CB_1 and D_{2L} increases in the presence of acute coactivation of both receptors (Kearn et al., 2005). Activation of either CB_1 or D_{2L} receptor individually did not significantly increase the physical association, suggesting that coactivation of both receptors is necessary for enhanced receptor dimerization. It was also reported that expression (and not activation) of the D_{2L} receptor was sufficient to induce a switch in CB_1-G protein coupling to a stimulatory pathway, however, measurements of the CB_1-D_{2L} receptor dimer were not performed (Jarrahian et al., 2004). In addition, another study reported a lack of agonist-mediated increase in the FRET interaction between CB_1 and D_2 receptors under conditions of both single and concurrent receptor activation (Marcellino et al., 2008). The lack of consistency between the reports described above may reflect differences in the choice of receptor ligands, the model systems, technical approaches, or the complex pharmacology of the CB_1-D_2 dimer.

In the present study, we used MBiFC to show that persistent activation of either the CB_1 or D_{2L} receptor leads to the formation of more CB_1-D_{2L} heterodimers relative to the D_{2L}-D_{2L} homodimers. There are several differences between our study of CB_1-D_{2L} interactions and the previous work described above (e.g., cell type, methods to measure receptors, drug treatment); however, the drug treatment conditions and technology used to assess the receptor dimers probably have significant influence. Each of the drug treatments reported here represents an extended drug exposure (i.e., 10–30 h). Drugs were added 4 h after transfection and were present during the time of ongoing receptor biosynthesis and subsequent oligomerization. Therefore, the dimers observed in our studies probably involve mechanisms not reflected in shorter drug treatments or acute studies (Kearn et al., 2005; Marcellino et al., 2008). The present study used BiFC technology, which differs from FRET in that the complementation of fluorescent signal is essentially irreversible (Vidi and Watts, 2009). This property of MBiFC allows investigators to "capture" and subsequently measure drug-induced changes in receptor dimers over an extended period in which a sufficient signal can be collected.

Persistent D_2 agonist treatment with quinpirole favored the formation of CB_1-D_{2L} heterodimers versus D_{2L}-D_{2L} homodimers. This effect was accompanied by an increase in D_{2L} receptor expression and was prevented by the D_2 antagonist sulpiride. The increase in D_{2L} receptor expression may suggest a pharmacological chaperone effect on receptor dimer formation where D_2 ligands stabilize the receptor, somehow promoting CB_1-D_{2L} receptor interactions (Vidi et al., 2008b). However, treatment with the D_2 antagonist sulpiride also

increased D_{2L} receptor density, but instead favored the formation of D_{2L}-D_{2L} homodimers. These opposing effects of D_2 agonists and antagonists on D_{2L}-D_{2L} versus CB_1-D_{2L} dimer formation argues against a simple role of increased D_{2L} receptor expression. One explanation for these differential effects may involve ligand-specific changes in receptor dimerization patterns (Vidi et al., 2008b). In addition to ligands, these dimerization patterns also appear to be influenced by the receptors under investigation. In a previous study of D_{2L} and A_{2A} receptor dimerization, quinpirole increased D_{2L}-D_{2L} homodimers relative to A_{2A}-D_{2L} heterodimers (Vidi et al., 2008b). The potential scenario gets increasingly complicated when considering a recent BiFC-BRET study providing evidence for a CB_1-D_2-A_{2A} receptor oligomer (Navarro et al., 2008). Linking the observations described above and the present results suggests a scenario where striatal neurons expressing D_{2L}, A_{2A}, and CB_1 receptors would be subject to a very complicated receptor regulation scheme. For example, persistent D_2 agonist treatment would increase overall D_{2L} receptor expression levels and perhaps promote the following pattern of receptor oligomers D_{2L}-$CB_1 > D_{2L}$-$D_{2L} > A_{2A}$-D_{2L}. The potential physiological and functional significance of these ligand-induced changes in heterodimers are intriguing and await biochemical and behavioral analysis (Marcellino et al., 2008). In addition to in vivo studies, new molecular tools to study these complex systems are becoming increasingly available as methods to study interactions of higher ordered GPCR oligomers (e.g., trimers and tetramers) such as BiLC-FRET, BiFC-FRET, and BiFC-BRET are developed (Vidi and Watts, 2009).

The ability of quinpirole to alter the formation of receptor oligomers involving D_{2L} receptors may provide insight into the disease states associated with persistent D_2 receptor activation, as in the treatment of Parkinson's disease with L-DOPA and D_2 dopamine receptor agonists (Hurley and Jenner, 2006). For example, persistent quinpirole treatment increases A_{2A}-A_{2A} homodimer formation and A_{2A} signaling (Vortherms and Watts, 2004; Vidi et al., 2008a). These observations may provide a molecular explanation for the beneficial clinical effects of A_{2A} antagonists in treating L-DOPA-induced dyskinesias (Morelli et al., 2007; Fuxe et al., 2008). The current results suggest that persistent treatment with D_2 receptor agonist drugs may promote the formation of CB_1-D_{2L} heterodimers. The increase in CB_1-D_{2L} dimer formation may allow the CB_1 receptor to have enhanced antagonistic effects over the D_2 receptor signaling (Marcellino et al., 2008). This scenario would provide for increased CB_1 signaling after a dopamine receptor-dependent increase in endocannabinoid release (Giuffrida et al., 1999; Piomelli, 2003). In addition, evidence linking the CB_1-D_{2L} heterodimer to a stimulatory pathway (Glass and Felder, 1997; Kearn et al., 2005) may provide a mechanism for CB_1 antagonism of D_2 signaling at the intracellular level (i.e., cAMP). Further in vivo investigations of CB_1 receptor and CB_1-D_{2L} heterodimer signaling after persistent D_2 receptor activation are warranted; however, studies suggest that the CB_1 receptor antagonists/inverse agonists may have beneficial effects in the management of Parkinson's disease. For example, the CB_1 antagonist 1-[7-(2-chlorophenyl)-8-(4-chlorophenyl)-2-methylpyrazolo[1,5-*a*]-[1,3,5]triazin-4-yl]-3-ethylaminoazetidine-3-carboxylic acid amide benzenesulfonate dose-dependently enhances the anti-Parkinson's activity of L-DOPA (Cao et al., 2007). Another study revealed that rimonabant, a CB_1 receptor inverse agonist, had beneficial effects in managing L-DOPA-induced dyskinesias (van der Stelt et al., 2005).

Similar to the D_{2L} receptors, the precise mechanism by which persistent activation of the CB_1 receptor favors the formation of CB_1-D_{2L} heterodimers relative to D_{2L}-D_{2L} homodimers remains largely unknown. Our observations suggest that the formation of the heterodimer is mediated by receptor activation and not alterations in CB_1 receptor expression. It is possible that the activated conformational state of the CB_1 receptor possesses enhanced affinity for the D_{2L} receptor and that persistent activation promotes CB_1-D_{2L} heterodimerization. This hypothesis is supported by the report that the CB_1 receptor increases the association with the D_{2L} receptor in a dose-dependent manner (Kearn et al., 2005). Furthermore, the present study demonstrated that expression of a constitutively active CB_1 mutant, CB_1T210I, promoted more CB_1-D_{2L} heterodimerization. Although the identification of a molecular mechanism awaits further study, it is tempting to consider that CB_1-D_{2L} interactions will represent a new CB_1 receptor signaling pathway that may be subject to functional selectivity (Glass and Northup, 1999; Mukhopadhyay and Howlett, 2005; Urban et al., 2007).

The physiological significance and functional consequences of CB_1 receptor-induced CB_1-D_{2L} dimers may have implications in the use of clinical cannabinoids to treat chronic pain as well as chronic marijuana use. Such conditions would involve persistent CB_1 receptor activation, providing an impetus to understand the molecular adaptations that occur in the nervous system (Cooper and Haney, 2008). Although we were able to study drug-induced changes of the CB_1-D_{2L} and D_{2L}-D_{2L} receptor dimers, a low BiFC signal between CB_1 receptors prevented us from examining the ratios of CB_1-CB_1 homodimers to CB_1-D_{2L} heterodimers. In the absence of CB_1-CB_1 studies, the CP55,940-induced increase in the CB_1-D_{2L} heterodimer may reflect a relative decrease in D_{2L}-D_{2L} homodimers and perhaps D_{2L} function. Consistent with this possibility we observed a modest CP55,940-induced decrease (approximately 15–25%) in D_{2L} receptor expression and D_{2L}-D_{2L} homodimers. These observations may suggest that persistent CB_1 receptor activation and subsequent CB_1-D_{2L} heterodimer formation could reduce D_{2L} receptor expression. In partial support of this hypothesis, it has been shown in rats and humans that chronic prenatal exposure to marijuana decreases the expression of dopamine D_2 receptors in the brain (Walters and Carr, 1986; Wang et al., 2004).

In the present report, we have visualized simultaneously the localization patterns of CB_1-D_{2L} heterodimers and D_{2L}-D_{2L} homodimers in living cells and provided evidence for agonist-regulated effects on receptor dimerization patterns. Recent studies propose that an increasing number of GPCRs may participate in higher order receptor oligomers or "receptor mosaics" and that these structures may mediate many signaling events (for review, see Fuxe et al., 2008). The present work and other recent studies are consistent with this concept (Carriba et al., 2008; Navarro et al., 2008). We anticipate the continued development of new technologies will allow investigators to examine these receptor mosaics in greater detail. Finally, the use of MBiFC provides a new tool to study drug-induced changes in receptor oligomerization and may offer an important asset relevant to the future of drug discovery in the area of receptor heterodimers.

Acknowledgments

We thank Dr. Karin Ejendal, Jason Conley, and Benjamin Chemel for careful reading of the manuscript and David Przybyla for assistance in preparing the figures.

References

Cao X, Liang L, Hadcock JR, Iredale PA, Griffith DA, Menniti FS, Factor S, Greenamyre JT, and Papa SM (2007) Blockade of cannabinoid type 1 receptors augments the antiparkinsonian action of levodopa without affecting dyskinesias in 1-methyl-4-phenyl-1,2,3,6-tetrahydropyridine-treated rhesus monkeys. *J Pharmacol Exp Ther* **323:**318–326.

Carriba P, Navarro G, Ciruela F, Ferré S, Casadó V, Agnati L, Cortés A, Mallol J, Fuxe K, Canela EI, et al. (2008) Detection of heteromerization of more than two proteins by sequential BRET-FRET. *Nat Methods* **5:**727–733.

Cooper ZD and Haney M (2008) Cannabis reinforcement and dependence: role of the cannabinoid CB1 receptor. *Addict Biol* **13:**188–195.

D'Antona AM, Ahn KH, and Kendall DA (2006) Mutations of CB1 T210 produce active and inactive receptor forms: correlations with ligand affinity, receptor stability, and cellular localization. *Biochemistry* **45:**5606–5617.

Fuxe K, Marcellino D, Rivera A, Diaz-Cabiale Z, Filip M, Gago B, Roberts DC, Langel U, Genedani S, Ferraro L, et al. (2008) Receptor-receptor interactions within receptor mosaics. Impact on neuropsychopharmacology. *Brain Res Rev* **58:**415–452.

Giuffrida A, Parsons LH, Kerr TM, Rodríguez de Fonseca F, Navarro M, and Piomelli D (1999) Dopamine activation of endogenous cannabinoid signaling in dorsal striatum. *Nat Neurosci* **2:**358–363.

Glass M and Felder CC (1997) Concurrent stimulation of cannabinoid CB1 and dopamine D2 receptors augments cAMP accumulation in striatal neurons: evidence for a G_s linkage to the CB1 receptor. *J Neurosci* **17:**5327–5333.

Glass M and Northup JK (1999) Agonist selective regulation of G proteins by cannabinoid CB(1) and CB(2) receptors. *Mol Pharmacol* **56:**1362–1369.

Glass M, Brotchie JM, and Maneuf YP (1997) Modulation of neurotransmission by cannabinoids in the basal ganglia. *Eur J Neurosci* **9:**199–203.

Herkenham M, Lynn AB, de Costa BR, and Richfield EK (1991) Neuronal localization of cannabinoid receptors in the basal ganglia of the rat. *Brain Res* **547:**267–274.

Herrick-Davis K, Egan C, and Teitler M (1997) Activating mutations of the serotonin 5-HT_{2C} receptor. *J Neurochem* **69:**1138–1144.

Hu CD, Chinenov Y, and Kerppola TK (2002) Visualization of interactions among bZIP and Rel family proteins in living cells using bimolecular fluorescence complementation. *Mol Cell* **9:**789–798.

Hu CD and Kerppola TK (2003) Simultaneous visualization of multiple protein interactions in living cells using multicolor fluorescence complementation analysis. *Nat Biotechnol* **21:**539–545.

Hurley MJ and Jenner P (2006) What has been learnt from study of dopamine receptors in Parkinson's disease? *Pharmacol Ther* **111:**715–728.

Jarrahian A, Watts VJ, and Barker EL (2004) D2 dopamine receptors modulate Gα-subunit coupling of the CB1 cannabinoid receptor. *J Pharmacol Exp Ther* **308:**880–886.

Kearn CS, Blake-Palmer K, Daniel E, Mackie K, and Glass M (2005) Concurrent stimulation of cannabinoid CB1 and dopamine D2 receptors enhances heterodimer formation: a mechanism for receptor cross-talk? *Mol Pharmacol* **67:**1697–1704.

Khan ZU, Mrzljak L, Gutierrez A, de la Calle A, and Goldman-Rakic PS (1998) Prominence of the dopamine D2 short isoform in dopaminergic pathways. *Proc Natl Acad Sci U S A* **95:**7731–7736.

Laviolette SR and Grace AA (2006) The roles of cannabinoid and dopamine receptor systems in neural emotional learning circuits: implications for schizophrenia and addiction. *Cell Mol Life Sci* **63:**1597–1613.

Leterrier C, Bonnard D, Carrel D, Rossier J, and Lenkei Z (2004) Constitutive endocytic cycle of the CB1 cannabinoid receptor. *J Biol Chem* **279:**36013–36021.

Marcellino D, Carriba P, Filip M, Borgkvist A, Frankowska M, Bellido I, Tanganelli S, Müller CE, Fisone G, Lluis C, et al. (2008) Antagonistic cannabinoid CB1/dopamine D2 receptor interactions in striatal CB1/D2 heteromers. A combined neurochemical and behavioral analysis. *Neuropharmacology* **54:**815–823.

Milligan G (2008) A day in the life of a G protein-coupled receptor: the contribution to function of G protein-coupled receptor dimerization. *Br J Pharmacol* **153 (Suppl 1):**S216–S229.

Morelli M, Di Paolo T, Wardas J, Calon F, Xiao D, and Schwarzschild MA (2007) Role of adenosine A2A receptors in parkinsonian motor impairment and l-DOPA-induced motor complications. *Prog Neurobiol* **83:**293–309.

Mukhopadhyay S and Howlett AC (2005) Chemically distinct ligands promote differential CB1 cannabinoid receptor-G_i protein interactions. *Mol Pharmacol* **67:**2016–2024.

Navarro G, Carriba P, Gandía J, Ciruela F, Casadó V, Cortés A, Mallol J, Canela EI, Lluis C, and Franco R (2008) Detection of heteromers formed by cannabinoid CB1, dopamine D2, and adenosine A2A G-protein-coupled receptors by combining bimolecular fluorescence complementation and bioluminescence energy transfer. *ScientificWorldJournal* **8:**1088–1097.

Pickel VM, Chan J, Kearn CS, and Mackie K (2006) Targeting dopamine D2 and cannabinoid-1 (CB1) receptors in rat nucleus accumbens. *J Comp Neurol* **495:**299–313.

Piomelli D (2003) The molecular logic of endocannabinoid signalling. *Nat Rev Neurosci* **4:**873–884.

Qi Y, Wang JK, McMillian M, and Chikaraishi DM (1997) Characterization of a CNS cell line, CAD, in which morphological differentiation is initiated by serum deprivation. *J Neurosci* **17:**1217–1225.

Shyu YJ, Liu H, Deng X, and Hu CD (2006) Identification of new fluorescent protein fragments for bimolecular fluorescence complementation analysis under physiological conditions. *Biotechniques* **40:**61–66.

Sibley DR and Neve KA (1997) Regulation of dopamine receptor function and expression, in *The Dopamine Receptors* (Neve KA and Neve RL eds) pp 383–424, Humana Press, Totowa, NJ.

Urban JD, Clarke WP, von Zastrow M, Nichols DE, Kobilka B, Weinstein H, Javitch JA, Roth BL, Christopoulos A, Sexton PM, et al. (2007) Functional selectivity and classical concepts of quantitative pharmacology. *J Pharmacol Exp Ther* **320:**1–13.

Usiello A, Baik JH, Rougé-Pont F, Picetti R, Dierich A, LeMeur M, Piazza PV, and Borrelli E (2000) Distinct functions of the two isoforms of dopamine D2 receptors. *Nature* **408:**199–203.

van der Stelt M, Fox SH, Hill M, Crossman AR, Petrosino S, Di Marzo V, and Brotchie JM (2005) A role for endocannabinoids in the generation of parkinsonism and levodopa-induced dyskinesia in MPTP-lesioned non-human primate models of Parkinson's disease. *FASEB J* **19:**1140–1142.

Vidi PA and Watts VJ (2009) Fluorescent and bioluminescent protein-fragment complementation assays in the study of G protein-coupled receptor oligomerization and signaling. *Mol Pharmacol* **75:**733–739.

Vidi PA, Chemel BR, Hu CD, and Watts VJ (2008a) Ligand-dependent oligomerization of dopamine D(2) and adenosine A(2A) receptors in living neuronal cells. *Mol Pharmacol* **74:**544–551.

Vidi PA, Chen J, Irudayaraj JM, and Watts VJ (2008b) Adenosine A(2A) receptors assemble into higher-order oligomers at the plasma membrane. *FEBS Lett* **582:**3985–3990.

Vortherms TA and Watts VJ (2004) Sensitization of neuronal A2A adenosine receptors after persistent D2 dopamine receptor activation. *J Pharmacol Exp Ther* **308:**221–227.

Walters DE and Carr LA (1986) Changes in brain catecholamine mechanisms following perinatal exposure to marihuana. *Pharmacol Biochem Behav* **25:**763–768.

Wang X, Dow-Edwards D, Anderson V, Minkoff H, and Hurd YL (2004) In utero marijuana exposure associated with abnormal amygdala dopamine D2 gene expression in the human fetus. *Biol Psychiatry* **56:**909–915.

Address correspondence to: Dr. Val J. Watts, Department of Medicinal Chemistry and Molecular Pharmacology, Purdue University, 575 Stadium Mall Dr., RHPH 210, West Lafayette, IN 47907-2091. E-mail: wattsv@purdue.edu